

Non-Destructive Qualification Testing for Aerospace Structures Using a Predictive Vibration Method

1st Samaher Shaheen

*Mechanical and Mechatronic Engineering
and Advanced Manufacturing Department
California State University, Chico
Chico, CA, USA
sshaheen@csuchico.edu*

2nd David Nguiffo

*Business Administration (MBA)
California State University, Chico
Chico, CA, USA
djnguiffo@csuchico.edu*

3rd Forest Siewert

*Mechanical and Mechatronic Engineering
and Advanced Manufacturing Department
California State University, Chico
Chico, CA, USA
fgsiewert@csuchico.edu*

4th Elizabeth E Rodriguez

*Computer Science Department
California State University, Chico
Chico, CA, USA
eerodriguez3@csuchico.edu*

5th Dennis M O'Connor

*Mechanical and Mechatronic Engineering
and Advanced Manufacturing Department
California State University, Chico
Chico, CA, USA
dmoconnor@csuchico.edu*

6th Yang Chao

*Mechanical and Mechatronic Engineering
and Advanced Manufacturing Department
California State University, Chico
Chico, CA, USA
ychao@csuchico.edu*

Abstract—Vibrational analysis is an important method for evaluating the structural performance of 3D-printed metal components in aerospace applications. Aerospace-grade materials are selected for their ability to resist extreme conditions, and their vibrational behavior must be carefully assessed to ensure reliability in challenging environments. This study examines the vibrational behavior of beams and complex geometries made from Inconel, a Nickel-Chromium Alloy known for its strength and heat resistance. In addition, other materials such as Titanium Alloys, Aluminum, and Stainless steel are considered due to their wide application in satellite construction. By introducing the Relative Frequency Shift (RFS) method, which employs vibrational and modal analysis to detect internal defects in 3D-printed metal components, a vast array of predicted responses can be frontloaded into a qualification procedure. This research incorporates machine learning (ML) to improve the organization and efficiency of prediction models and automate defect identification. ML algorithms analyze large datasets to uncover patterns related to voids, cracks, or other irregularities that can occur during the 3D printing process. With ML integration, the study speeds up vibrational analysis, enhances accuracy, and reduces the reliance on physical testing, allowing for faster transitions from design to production. Using Ansys simulation and the finite element method (FEM), modal and harmonic analyses are conducted, incorporating Timoshenko beam theory to account for shear deformation and rotary inertia. The Timoshenko theory is integrated into an algorithm that helps detect potential defects, such as voids or deformations, which may arise during the 3D printing process. Timoshenko beam theory offers a significant advantage over different models, which are crucial for accurately analyzing components with non-uniform geometries. This level of detail ensures that even indistinct internal deformations are captured, providing deeper insights into the material behavior under dynamic conditions. The integration of Timoshenko theory into FEM simulations allows for more realistic and practical results, bridging the gap between theoretical analysis and real-world applications. Ansys, as the chosen simulation platform, excels in handling complex geometries and multi-material assemblies, enabling the study to precisely replicate the operational environment of aerospace components. By leveraging Ansys' advanced capabilities, the study ensures that all potential scenarios, including thermal expansion and vibrational loads, are accurately modeled, leading to more reliable predictions and safer designs.

Current testing methods for aerospace components often involve extensive physical experiments, including vibration tables, thermal cycling chambers, and destructive testing to

evaluate failure points. While these methods provide valuable insights, they are time-consuming, costly, and limited in their ability to explore a wide range of scenarios. This study integrates advanced simulations and predictive algorithms to examine 3D-printed parts through vibrational analysis, FEM simulation, and theoretical modeling. It offers a complementary approach that reduces dependency on exhaustive physical tests while maintaining accuracy and reliability to understanding material behavior.

Predictive methods powered by ML detect potential flaws early, cutting down on delays and preventing material waste as well as preventing possible failure. By identifying natural frequencies and mode shapes, engineers can confirm that components meet performance criteria under operational conditions. The added accuracy from ML-driven insights strengthens these evaluations, making it easier to identify structural weaknesses before they affect performance. This tool not only enhances technical reliability but also supports supply chain efficiency by reducing production errors, minimizing waste, and improving part quality. These findings help aerospace companies streamline their supply chains, lower manufacturing costs, and ensure more reliable, high-performing components for satellite structures, meeting the demanding conditions of space. Collaboration between suppliers and manufacturers improves significantly when shared data and tools are utilized. This approach allows for a supply chain that adapts easily to changes and responds quickly to demands. By addressing current challenges in aerospace production, it also establishes a foundation for future innovation, helping the industry stay ahead and meet the requirements of space exploration.

Keywords—*Vibration, Qualification Testing, Non-destructive Testing, Additive Manufacturing, Manufacturing Defects, Modal Analysis.*

I. INTRODUCTION

The increasing reliance on additive manufacturing (AM) in aerospace engineering has introduced both new capabilities and new challenges, particularly in the qualification as the industry adopts complex 3D-printed geometries and high-performance alloys. Metal components fabricated using AM, such as selective laser melting (SLM) and electron beam melting (EBM), often feature complex geometries, internal residual stresses, and variations in microstructure [1]. These characteristics can have a significant impact on mechanical

behavior and structural integrity under dynamic or loading conditions. Reliable non-destructive qualification methods are therefore needed to verify that components meet aerospace performance standards without relying on time-consuming or destructive testing procedures [2].

AM enables the production of aerospace components with complex geometries that difficult to achieve through conventional methods. Materials such as Inconel, Titanium Alloys, Aluminum, and Stainless Steel are commonly used for their strength-to-weight efficiency and ability to perform under extreme thermal and mechanical environments [3]. These material characteristics are important in applications such as satellite structures, and other high-performance aerospace assemblies. However, the layer-by-layer nature of 3D printing fabrication can introduce sub-surface defects such as lack of fusion, internal porosity, and residual thermal stress that are not easily detected through visual or surface inspection [4]. Ensuring component quality requires methods capable of detecting internal defects without altering or damaging the part.

Aerospace manufacturing commonly uses several non-destructive testing (NDT) methods, including ultrasonic inspection, X-ray radiography, thermographic imaging, eddy current probing, and magnetic particle testing. While these techniques are well established in the industry, each presents specific limitations depending on the material, geometry and type of defect being tested. For example, Radiographic inspection requires safety precautions, is costly to operate, and may struggle with resolution in high-density materials [5]. Surface-sensitive methods like eddy current and magnetic particle inspection are not effective for internal flaws and require materials with specific electromagnetic properties [6]. Beyond technical limitations, these techniques often require specialized tools, trained operators, and controlled testing environments. That makes these requirements expensive and difficult to implement in production lines. The need for frequent calibration, inspection time, and post-processing further contributes to increase overall production costs and delay delivery schedules, particularly in high-mix, low-volume production common to space-grade components [7].

These challenges have motivated the development of alternative approaches that preserve the benefits non-destructive testing, cost-efficient, scalability, and adaptable to the unique characteristics of AM [8]. This paper investigates vibrational analysis as a qualification method for 3D-printed aerospace components. By analyzing shifts in dynamic response and characteristics, such as changes in natural frequencies and mode shapes, internal defects can be identified through their effect on stiffness and mass distribution. Often caused by internal defects such as voids, these variations of this nature, offer a reliable basis for evaluating structural integrity [9]. Vibrational analysis is a widely applied method for examining how structures respond to dynamic loading. It focuses on identifying natural frequencies and mode shapes, which are directly influenced by the distribution of mass and stiffness within a component [10]. Any disturbance to this balance, such as internal defects, can lead to measurable changes in the vibrational response, making it a useful tool for detecting structural inconsistencies without direct access to the interior [11]. This approach is based on Relative Frequency Shift (RFS), which measures percentage changes in natural frequencies relative to a component without defects. RFS allows internal voids to be

detected by tracking changes in the natural frequencies of the beam. The presence of a void affects how vibrations travel through the structure, resulting in small but measurable shifts in frequency [12]. Combined with Ansys simulation and machine learning predictive modeling, this approach helps improve quality assurance without adding significant cost or time to the production process.

To accurately capture the dynamic behavior of 3D-printed aerospace components, this study utilizes Timoshenko beam theory. This theory includes shear deformation and rotary inertia, which are important for analyzing both basic beams and thin-walled tubes, where dynamic behavior can be affected by internal defects [13]. Thin-walled tubes have different cross-sectional properties from solid rectangular beams, these properties significantly affect their moment of inertia. In tubular sections, both the outer and inner radii influence the moment of inertia, making them more sensitive to changes in wall thickness and internal defects [14]. Accurately modeling these properties is important for predicting vibrational behavior and identifying changes that may indicate structural flaws and defects. Ansys is a commonly used simulation platform in aerospace design and analysis, known for its ability to handle complex geometries and boundary conditions. It includes Timoshenko beam theory in its standard formulation, making it suitable for evaluating structural response under dynamic loading [15]. The finite element method (FEM) enables precise modeling of stress distribution, deformation, and vibrational modes, providing insight into how internal voids or material inconsistencies can affect the way 3D-printed components respond to dynamic loads [16]. The simulation results provide a baseline for understanding how defect location and geometry influence vibrational behavior of the structure. By monitoring variations in its natural frequencies. RFS occur when there are changes in stiffness or mass distribution, which can result from internal flaws such as voids or cracks [17].

To validate the simulation work, a mathematical model based on Timoshenko beam theory was developed and used to generate training data for a machine learning algorithm. This model included various defect scenarios by adjusting the location of voids in both beam and tube configurations. First introduced by Stephen Timoshenko in the early 1920s, the theory addressed limitations in classical beam models by incorporating both transverse shear deformation and rotary inertia [18]. As a result, it offers improved accuracy in vibration analysis, where even small modeling differences can significantly influence predicted natural frequencies [19]. The output data allowed the algorithm to learn how these internal changes affect stiffness, mass distribution, and resulting frequency shifts. Using machine learning makes it possible to relate these shifts to specific defect conditions, allowing for faster detection and improved consistency across different structural configurations [20]. The RFS values obtained from both the theoretical and simulated models were compared and assembled into a database enabling the correlation of specific frequency shifts with corresponding defect locations. This method enables defect detection across different geometries by using machine learning trained on a structured collection of simulation and theoretical data.

Recent research has shown that machine learning (ML) can enhance vibration analysis by enabling fast and data-driven prediction of beam behavior. Regression-based machine learning models have been used to predict the natural

frequencies of various beam types, demonstrating high accuracy and reduced computational demands [21]. Similarly, machine learning techniques have been applied to predict the deflection and shape of 2D cantilever beams, validating the capability of these models for structural behavior prediction [22].

In the context of damage detection, several studies have implemented machine learning techniques to identify defects such as cracks in cantilever beams, which are often challenging to detect using conventional analytical or visual inspection methods. A correlation-based ML approach has been used for crack detection, highlighting its potential in structural health monitoring [23]. Another investigation applied both regression and machine learning models to identify damage in cantilever beams, further demonstrating the reliability of data-driven methods in structural diagnostics [24]. Additionally, vibration-based features such as frequency response functions (FRFs) and time-frequency signatures have been integrated with machine learning classifiers for more advanced damage detection frameworks. A hybrid method combining FRFs with machine learning has been proposed to detect structural damage [25]. On the other hand, deep learning approaches using time-frequency extended signatures have also been applied for beam condition monitoring, demonstrating the effectiveness of deep models in identifying subtle dynamic anomalies [26].

Previous studies provide a strong foundation for the use of machine learning in structural dynamics. They also motivate the development of a hybrid approach that combines Timoshenko beam theory with Artificial Neural Networks (ANNs) to predict the vibrational behavior of beams and complex geometries fabricated from aerospace-grade materials. ANNs are effective for this purpose due to their ability to model complex, nonlinear relationships between structural properties and vibrational response [27].

By integrating Timoshenko theory in both simulation and algorithmic modeling, this study establishes a consistent and reliable approach for non-destructive qualification method. The combined use of finite element analysis and machine learning enables early detection of internal defects in 3D-printed aerospace components, whether simple or geometrically complex.

Machine learning, particularly using artificial neural networks, has shown increasing promise in vibration-based structural assessment. This study builds on that work by applying similar techniques to aerospace materials, where accurate vibration response is essential for safety and performance. Through automated detection of internal defects, such as voids, or irregularities introduced during additive manufacturing. This approach provides a practical and scalable tool for structural evaluation in aerospace applications.

II. MATERIALS AND METHODS

A. Materials and Geometries

This study investigates two structural configurations: a solid rectangular beam Fig. 1 and a thin-walled cylindrical tube Fig. 2.

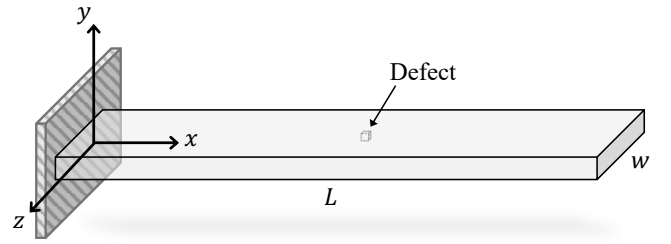


Fig. 1: Fixed-Free beam with an internal defect.

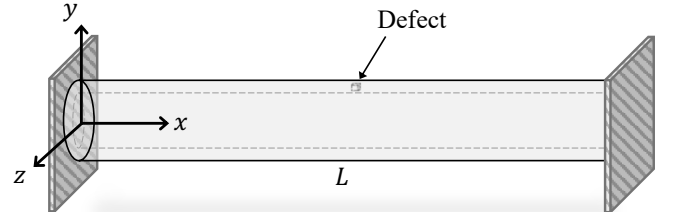


Fig 2: Fixed-Fixed thin-wall tube with an internal defect.

These geometries were selected to represent both simple and more complex structural forms that are common in aerospace components.

The materials used in this study consist of commonly used aerospace-grade alloys, which were chosen based on their performance under extreme mechanical and thermal conditions. The following materials were investigated:

Table 1: Materials Properties

Material	Density	E-Modulus
Inconel 718	8070 kg/m ³	220 GPa
Stainless Steel 316	7910 kg/m ³	180 GPa
Titanium Ti6Al4V	4360 kg/m ³	110 GPa
Aluminum	2590 kg/m ³	70 GPa

Inconel 718 was selected as the base material for both models due to its common use in aerospace applications. Known for its high strength, corrosion resistance, and stability at elevated temperatures, Inconel provides a suitable representation of 3D-printed, aerospace certified components.

Internal defects were introduced as a square-shaped void located at different locations along the length and width of the beam. The voids were modeled as a square cross-sectional, reducing stiffness and mass. For the tube geometry, the void was also modeled with a square cross-sectional located at different locations along the length. The void was oriented to follow the curvature of the cylindrical wall, mimicking defects that may result from incomplete fusion along the printing process.

A total of 21 cases were generated for each geometry and material, including range of defect locations along both structures. The void locations for the beam and tube configurations are listed in Table 2 and Table 3, respectively. These tables define the locations where the square-shaped void was introduced for each case.

Table 2: Beam Void Locations

Parameter	Value (m)
x_1	0.074
x_2	0.130
x_3	0.220
z_0	0
z_1, z'_1	0.00127
z_2, z'_2	0.00508
z_3, z'_3	0.00889

Where x_n is the location of the void along the length of the beam L from the fixed end. The z_0 is the location of the void in the middle-width of the beam, and z_n, z'_n is the location of the void from the edge of the beam along the width w .

Table 3: Tube Void Locations

Parameter	Value (m)
x_1	0.015
x_2	0.06
x_3	0.105
x_4	0.15
x_5	0.195
x_6	0.24
x_7	0.285

Where x_n is the location of the void along the length of the tube L from the left fixed end.

B. Methods

Modal and harmonic analyses were conducted using Ansys Mechanical, with both geometries. The beam was modeled with a fixed-free boundary conditions, which was used to represent a 3D-printed testing coupon and to validate the method using a simple structural configuration. The tube geometry was analyzed under fixed-fixed boundary conditions to represent a more complex geometry relevant to aerospace components. As Ansys applies Timoshenko beam theory, which accounts for both shear deformation and rotary inertia. The software was used to simulate a range of defect scenarios across different geometries, allowing for systematic evaluation of how void location influence vibrational behavior. For each case, natural frequencies and mode shapes were recorded for both the intact and defected models. The introduction of the void affected the local stiffness and mass, which caused shifts in the vibrational response. These shifts were measured using the RFS, defined as:

$$RFS = \frac{f_0 - f_d}{f_0} \quad (1)$$

Where f_0 is the natural frequency of the intact model, and f_d is the natural frequency of the model with void.

By comparing frequency results from defective and non-defective models, the Relative Frequency Shift (RFS) was computed to measure the impact of each defect configuration.

The RFS value was used as the main indicator for detecting the defect location.

A theoretical model based on Timoshenko beam theory was developed and applied to the beam configurations to validate the simulation results from Ansys. The model used the same material properties, geometry, and boundary conditions as those defined in the finite element setup. Square-shaped voids were treated as localized reductions in cross-sectional stiffness and mass, enabling the computation of natural frequencies for each defect scenario.

This model focuses exclusively on transverse vibration modes, which are the most sensitive to internal stiffness and mass changes. The theoretical basis is established using the governing differential equations of Timoshenko beam theory are:

$$\rho A \frac{\partial^2 \omega(x,t)}{\partial t^2} = \frac{\partial}{\partial x} \left[kGA \left(\frac{\partial^2 \omega(x,t)}{\partial x^2} - \phi(x,t) \right) \right] \quad (2)$$

$$\rho A \frac{\partial^2 \omega(x,t)}{\partial t^2} = \frac{\partial}{\partial x} \left(EI \frac{\partial \phi(x,t)}{\partial x} \right) + KGA \left(\frac{\partial \omega(x,t)}{\partial x} - \phi(x,t) \right) \quad (3)$$

In these equations, $\omega(x,t)$ represents the transverse displacement of the beam, and $\phi(x,t)$ denotes the rotation of the cross-section. The parameters include E for Young's modulus, G for the shear modulus, ρ for material density, A for the cross-sectional area, I for the second moment of area, and K as the shear correction factor.

The shear modulus G , which governs the material's resistance to shear deformation, is related to Young's modulus and Poisson's ratio ν by the expression:

$$G = \frac{E}{2(1+\nu)} \quad (4)$$

This relationship is used to determine the shear stiffness term KGA , which is included in both the stiffness matrix and the governing equations. For a beam with a rectangular cross-section, the second moment of area is calculated as:

$$I = \frac{bh^3}{12} \quad (5)$$

where b is the width and h is the height of the beam cross-section. This geometric property directly affects the bending stiffness and the natural frequencies of the structure. When a square-shaped void is introduced, it reduces both the cross-sectional area and the moment of inertia of the section. In the case where the void is not centered on the neutral axis, its contribution to the moment of inertia is calculated using the parallel axis theorem:

$$I_{void} = \frac{a^4}{12} + Ad^2 \quad (6)$$

where a is the length of the void, A is its area, and d is the distance from the void's center to the neutral axis. This value is subtracted from the original moment of inertia to account for the local reduction in stiffness.

This theoretical model was implemented in MATLAB using a finite element approach. Natural frequencies were computed for both intact and defected beam configurations, and only transverse modes were recorded. These results were then compared with Ansys simulations to verify consistency between both methods.

To support the machine learning structure and improve compatibility with data processing tools, the original MATLAB implementation was rewritten in Python. The same finite element formulation was maintained to ensure that the natural frequency results remained consistent with those previously obtained. Each case was defined by material properties, beam geometry, void location, and computed frequencies, and recorded in a structured database.

Using Python allowed direct integration with data handling libraries and machine learning workflows. For each configuration, the RFS was calculated based on the difference between the frequencies of the intact and defected models. These values were stored alongside the corresponding input parameters, creating the dataset used to train and assess the machine learning model. This transition to Python also improved the efficiency of batch processing for multiple defect scenarios and simplified the overall workflow.

Modal frequencies, mode shapes, and damping characteristic were extracted from the simulations. The dataset included geometric parameters (length, width, thickness), materials properties (Young's modulus, density, Poisson's ratio), and resulting vibrational responses. These were compiled into a structured database used for training the machine learning model.

ANN model was developed to predict the vibrational characteristics of the structures based on their input parameters. ANN was selected for its ability to model complex nonlinear relationships between structural properties and vibrational behavior.

III. RESULTS

Natural frequencies describe how a structure responds when set into vibration and it depend on its shape, material, and how it's supported. If the structure has an internal change like a defect or variation in stiffness, its natural frequencies can shift. Four different AM materials were tested, Inconel, Stainless Steel, Aluminum, and Titanium. Understanding how the materials modal response varies between material properties is key to detecting a void defect. The void used in the analysis had a very small size relative to the beam, this led to the magnitude of the percentage of frequency shift being relatively small.

The third mode was selected for analysis because it provides a more detailed deformation pattern than the fundamental or second modes. While the first mode generally shows a single smooth curvature, the third mode introduces multiple peaks and inflection points along the beam. These variations in displacement make it more effective for evaluating how internal defects influence vibrational response. Defects located near antinodes, where displacement is greatest, tend to cause more noticeable shifts in natural frequency. This makes the third mode particularly suitable for studying the influence of void position on vibrational response.

From Fig. 3 below, it can be observed that this natural frequency shift for three of the materials is maximal near the edges of the beam and drops as the void's location nears the mid-width of the beam, where it reaches its minimum value. This behavior may be explained by the bending stresses being maximal towards the edges of the beam and drops to a minimum value towards its middle.

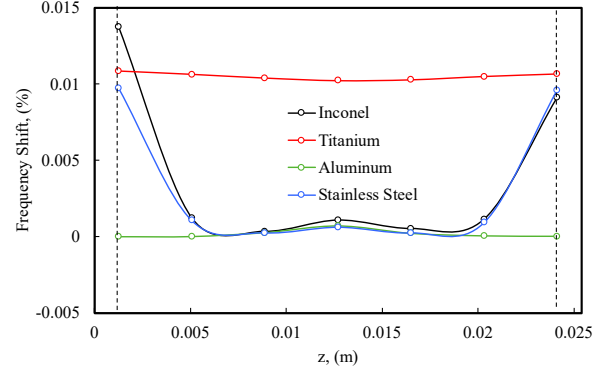


Fig. 3: 3rd-mode frequency shift for all materials with a void at location ($z = 0.074m$) along the beam length.

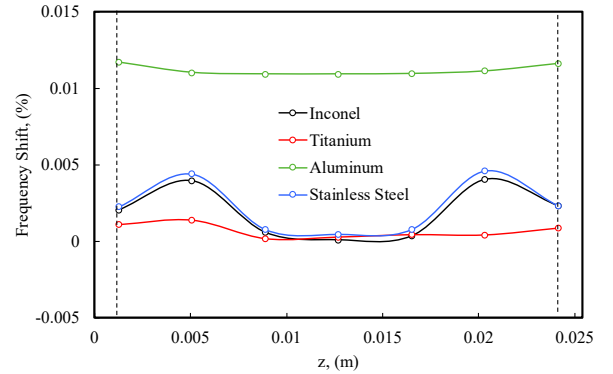


Fig. 4: 3rd-mode frequency shift for all materials with a void at location ($z = 0.13m$) along the beam length.

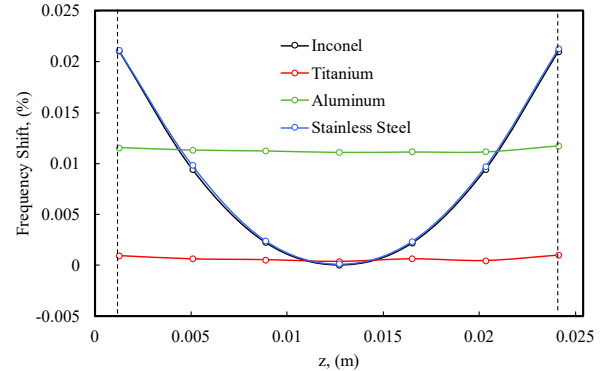


Fig. 5: 3rd-mode frequency shift for all materials with a void at location ($z = 0.22m$) along the beam length.

Moreover, for Inconel and Stainless Steel beams, the percentage of the frequency shift is greater at third location than at the first location. Considering that the voids at the first location all lie on the first antinode of the third mode of vibration, where the displacement of the beam is close to its maximum value, this result was expected. However, the fact that the voids at the third location all lie on the third node of the third mode of vibration was unexpected. The presence of

a void at an antinode, where the beam reaches its highest displacement during vibration, would be expected to significantly alter the mass distribution and stiffness of the beam, resulting in a maximal frequency shift for all materials at that location. In contrast, a void located at the third node of vibration, where the beam experiences minimal vibration during its response, was expected to have a negligible impact on the natural frequencies of the beam, resulting to relatively small frequency shifts. However, this outcome was observed only in the Titanium beam, while other materials showed more noticeable deviations.

The beam results provide a clear view of how frequency shifts vary across different materials. As shown in Fig. 6 Inconel and Stainless Steel exhibits the highest percentage frequency shift near the edges of the beam. Across the rest of the beam's width, Titanium shows the greatest frequency shift among the four materials tested. In Fig. 7, at the second location, the Aluminum beam shows the highest percentage frequency shift across the width of the beam. In Fig. 8, at the third location, both Inconel and Stainless Steel yield the largest shift in natural frequency. Given that all geometries and boundary conditions remained constant, with material properties as the only varying factor, the variation in which material yielded the maximum frequency shift is notable. One would expect a consistent trend in the material producing the highest shift across all void locations; however, the results indicate a more location-dependent response. A consistent trend in the material exhibiting the highest percentage frequency shift across all transverse void locations would typically be anticipated based on material stiffness and density characteristics.

To further explore this behavior, the ratio of Young's modulus to density was evaluated, as it is known to influence natural frequency. The goal was to determine whether this ratio could explain the observed differences in frequency shifts. However, no consistent relationship was found between the modulus-to-density ratio and the magnitude of the frequency shifts. Although the modulus-to-density ratio provides general insight into dynamic behavior, it did not explain why some materials exhibited larger shifts than others when all structural and loading variables were controlled. This suggests that the interaction between material properties and localized defects may involve more complex mechanisms. As the way internal stresses or energy distribution respond to discontinuities is not fully captured by the global stiffness-to-mass ratio, it suggests that additional material-specific factors influence the vibrational response to localized defects, even under controlled structural and boundary conditions.

Both the theoretical results from MATLAB and the simulation data from Ansys exhibit a symmetric pattern in the percentage frequency shift across the beam width for Inconel 718 under the third vibrational mode, as shown in the figures corresponding to void locations at ($z = 0.074m$) Fig. 6, ($z = 0.13m$) Fig. 7, and ($z = 0.22m$) Fig. 8. These represent void locations 1, 2, and 3, respectively, along the beam's length.

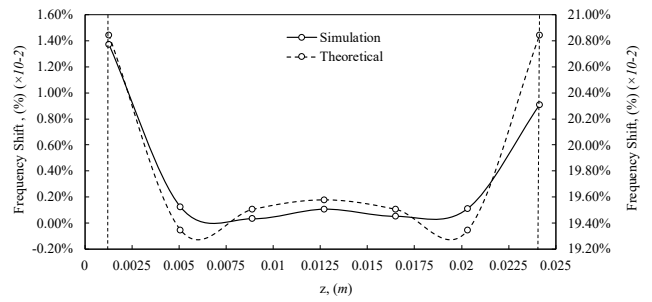


Fig. 6: Absolute frequency shift percentage for the 3rd-mode at location ($z = 0.074m$) along the beam length.

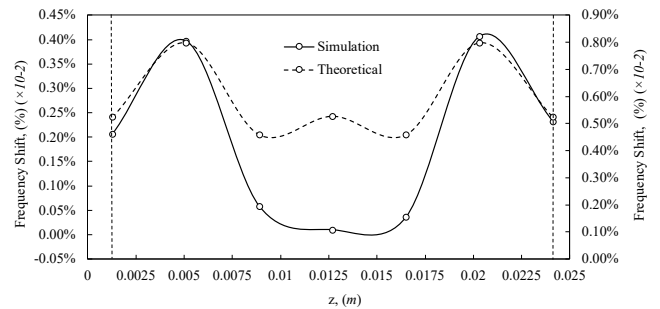


Fig. 7: Absolute frequency shift percentage for the 3rd-mode at location ($z = 0.13m$) along the beam length.

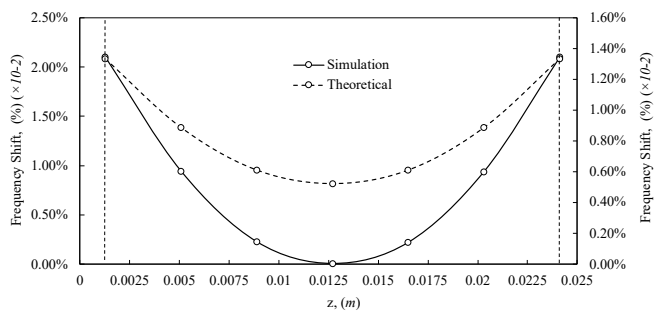


Fig. 8: Absolute frequency shift percentage for the 3rd-mode at location ($z = 0.22m$) along the beam length.

In all three locations, the theoretical predictions from MATLAB tend to yield slightly higher frequency shifts compared to the Ansys Mechanical. At the second location Fig. 7, the theoretical results show a peak shift near the mid-width of the beam, while the Ansys data reflect a more uniform distribution with minimal variation across the width.

This difference can be attributed to the fundamental distinction in how each method approaches the problem. The MATLAB model is based on a direct mathematical implementation of Timoshenko beam theory. It solves the governing differential equations analytically and treats the void as a localized reduction in stiffness and mass, incorporated through changes in the moment of inertia and cross-sectional area. In contrast, Ansys relies on finite element analysis, where the geometry is discretized into individual elements and solved numerically using interpolation functions and matrix assembly. The way Ansys handles mesh density, shape functions, and numerical integration may smooth out localized effects, especially if the mesh is not highly refined around the void region. As a result, the simulation may

underpredict frequency shifts compared to the more idealized analytical model.

To further illustrate the influence of the void defect placement, Fig. 9 presents a surface plot of the third-mode frequency shift distribution for Inconel 718, covering all 21 void locations across the beam. The frequency response is shown along both the length and width, reflecting how changes in void location affect the natural frequency. As observed, the largest shifts occur near the free end and along the outer edges of the beam, where vibrational displacement is highest. This pattern highlights the sensitivity of the third mode to void location and supports the earlier finding that frequency response is strongly influenced by local deformation characteristics.

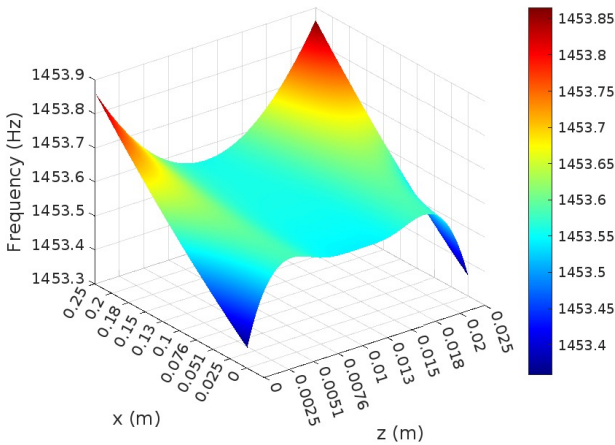


Fig. 9: 3rd-mode frequency shift surface plot for Inconel beam.

Ansys Mechanical was also used to calculate the modal response for the complex tube geometry. This followed the validation step in which Ansys results for the beam were compared against theoretical predictions obtained from the MATLAB implementation of Timoshenko beam theory. The close agreement between the two confirmed the accuracy of the finite element approach used by Ansys Mechanical to solve for the structure's modal response. This validation supports its use for analyzing more complex structural configurations, such as the tube.

Considering a complex geometry, Fig. 10 illustrates the shift in the third mode natural frequency of an Inconel tube. The model demonstrated a significant frequency shift across all seven void locations, indicating a distinct response when a void is present.

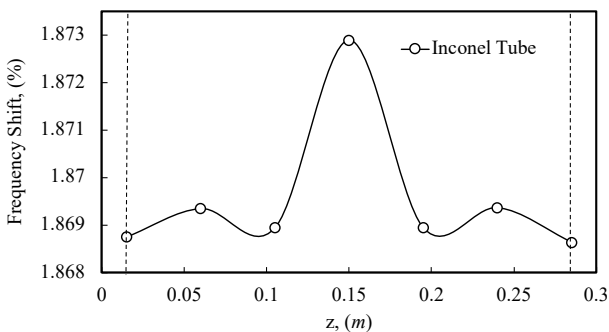


Fig. 10: 3rd-mode frequency shift for Inconel tube.

Fig. 10 and Fig. 11 illustrate a symmetric response along the tube's length, which is consistent with the expected behavior of a fixed-fixed boundary condition. Fig. 11 displays the fourth vibrational mode, which is the inverse of the third mode in terms of displacement profile. This mode introduces an additional node along the length, resulting in alternating regions of maximum and minimum displacement. The symmetry observed in both plots is influenced by the even spacing of voids along the tube, which affects the local stiffness without disrupting the overall modal shape. These results indicate that the model effectively captures the dynamic characteristics of the structure.

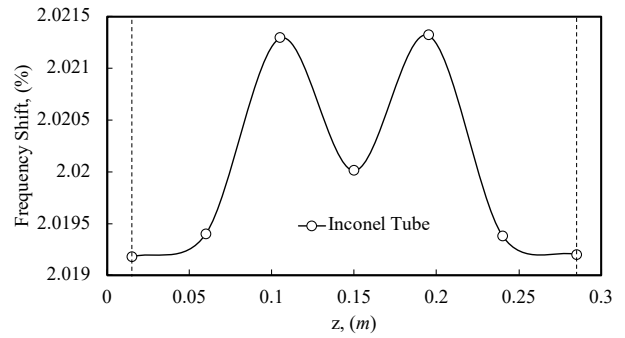


Fig. 11: 4th-mode frequency shift for Inconel tube.

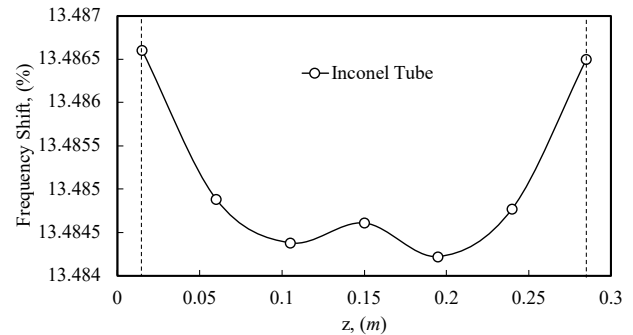


Fig. 12: 8th-mode frequency shift for Inconel tube.

In the higher natural frequency modes, the tubular geometry exhibits a distinct shift in its natural frequencies. The fourth and eighth mode of vibration was selected to demonstrate this effect, as shown in Fig.10 and Fig. 11. Fig. 12 shows the frequency shift for the eighth mode of the Inconel tube. This thin-walled geometry introduces added sensitivity to local stiffness changes, making it especially responsive to internal defects. The eighth mode includes more nodes and inflection points, producing a complex deformation pattern along the length of the tube. In higher modes like this, even small voids can influence the dynamic response, as the vibration shape interacts with localized mass and stiffness variations. In fixed-fixed structures, the symmetry of the boundary conditions helps maintain a balanced modal distribution, but the effect of defects remains visible. These shifts in frequency provide a practical means for identifying the presence of voids in AM components, where surface inspection may not reveal subsurface inconsistencies.

To evaluate its predictive performance, the trained ANN was used to estimate the natural frequencies from structural and material inputs. The model effectively captured the relationship between defect characteristics and frequency response, providing accurate predictions across different

configurations. The ANN architecture included an input layer corresponding to the normalized features, followed by three hidden layers with 128, 64, and 32 neurons. Each hidden layer used ReLU activation, batch normalization, and dropout for regularization. The output layer employed a linear activation function to predict continuous-valued natural frequencies

The model was trained using the Adam optimizer with a learning rate scheduler, and the loss function was defined as mean squared error (MSE) to minimize deviations from simulation outputs. Preprocessing steps included input normalization, principal component analysis (PCA) for dimensionality reduction, and noise filtering of simulation data. The dataset was divided into training (80%), validation (10%), and testing (10%). Hyperparameters tuning was conducted through grid search and cross-validation, adjusting the number of layers, neurons, dropout rates, and batch size. The machine learning outcomes from the training set are as follows:

Table 4: Machine Learning Outcome

Material	Prediction Accuracy (%)	MSE (%)
Inconel 718	84.59	2.39
Stainless Steel 316	84.0	6.00

Model evaluation showed an average prediction accuracy of 84.0% with a MSE of 6.0% for Stainless Steel and 84.59% and 2.39% respectively, for the Inconel. While these results suggest the model is off to a promising start in identifying patterns between structural parameters and vibrational responses, they also indicate room for improvement. Expanding the dataset and refining data quality could help enhance future model performance.

The combination of Timoshenko beam theory, finite element analysis, and machine learning offers a reliable and efficient approach for evaluating the vibrational behavior of 3D-printed aerospace structures. By integrating analytical modeling with numerical simulation and predictive algorithms, the method enhances defect detection while also providing meaningful insight into how internal variations affect structural response. It enables the prediction of expected vibrational patterns, highlights areas where deviations are likely to occur, and guides attention to regions that may require further inspection. This makes the approach well suited for early-stage qualification and reduces reliance on extensive physical testing in the assessment of complex aerospace components.

ACKNOWLEDGMENT

We would like to thank and acknowledge the Department of Mechanical and Mechatronic Engineering and Advanced Manufacturing at California State University, Chico, as well as the broader university leadership, for their continued support of our research efforts.

REFERENCES

- [1] Froes, F. H., & Boyer, R. (2019). *Additive Manufacturing for the Aerospace Industry* (1st ed.). Elsevier.
- [2] D. Wu, W. Qu, Y. Wen, Y. Zhang, and B. Liang, "The application, challenge, and developing trends of non-destructive testing technique for large-scale and complex engineering components fabricated by metal additive manufacturing technology in aerospace," *J. Nondestruct. Eval.*, vol. 43, no. 3, 2024. [Online]. Available: <https://doi.org/10.1007/s10921-024-01107-3>
- [3] I. V. Shishkovsky, *Additive Manufacturing of High-performance Metals and Alloys: Modeling and Optimization*. London, U.K.: IntechOpen, 2018. [Online]. Available: <https://doi.org/10.5772/intechopen.69421>
- [4] G.-R. Gillich, N. M. M. Maia, M. A. Wahab, C. Tufisi, Z.-I. Korka, N. Gillich, and M. V. Pop, "Damage detection on a beam with multiple cracks: A simplified method based on relative frequency shifts," *Sensors*, vol. 21, no. 15, p. 5215, 2021. [Online]. Available: <https://doi.org/10.3390/s21155215>
- [5] S. Lampman, M. Mulherin, and R. Shipley, "Nondestructive testing in failure analysis," *J. Fail. Anal. Prev.*, vol. 22, pp. 66–97, 2022. [Online]. Available: <https://doi.org/10.1007/s11668-021-01325-1>
- [6] S. Kim, J. K. Seo, and T. Ha, "A nondestructive evaluation method for concrete voids: Frequency differential electrical impedance scanning," *SIAM J. Appl. Math.*, vol. 69, no. 6, pp. 1759–1771, 2009. [Online]. Available: <http://www.jstor.org/stable/27798756>
- [7] Z. Hong-ping, H. Bo, and C. Xiao-qiang, "Detection of structural damage through changes in frequency," *Wuhan Univ. J. Nat. Sci.*, vol. 10, no. 6, pp. 1069–1073, 2005. [Online]. Available: <https://doi.org/10.1007/bf02832469>
- [8] Z. L. Gan, S. N. Musa, and H. J. Yap, "A review of the high-mix, low-volume manufacturing industry," *Applied Sciences*, vol. 13, no. 3, p. 1687, 2023. [Online]. Available: <https://doi.org/10.3390/app13031687>
- [9] P. Y. Papalambros and D. J. Wilde, *Principles of Optimal Design: Modeling and Computation*, 2nd ed. Cambridge, U.K.: Cambridge Univ. Press, 2000. [Online]. Available: <https://doi.org/10.1017/CBO9780511626418>
- [10] S. Shaheen, D. J. Nguiffo, E. E. Rodriguez, F. G. Siewert, and D. M. O'Connor, "Investigating the influence of a laterally placed void on natural frequency shifts using Timoshenko beam theory," presented at the ASME Aerospace Structures, Structural Dynamics, and Materials Conf. (SSDM 2025), Houston, TX, USA, May 2025.
- [11] S. S. Rao, *Mechanical Vibrations*, 4th ed. Upper Saddle River, NJ, USA: Pearson Prentice Hall, 2004.
- [12] Gao, W. et al., "The status, challenges, and future of additive manufacturing in engineering," *Comput.-Aided Design*, vol. 69, pp. 65–89, 2015. [Online]. Available: <https://doi.org/10.1016/j.cad.2015.04.001>
- [13] S. Timoshenko, *Vibration Problems in Engineering*. New York, NY, USA: Van Nostrand, 1961.
- [14] S. P. Timoshenko, "LXVI. On the correction for shear of the differential equation for transverse vibrations of prismatic bars," *The London, Edinburgh, and Dublin Philosophical Magazine and Journal of Science*, vol. 41, no. 245, pp. 744–746, May 1921, doi: <https://doi.org/10.1080/14786442108636264>
- [15] Jiang, J., Wang, L., & Wang, X. (2019). Differential Quadrature Element Method for Free Vibration of Strain Gradient Beams with Elastic Boundary Conditions. *Journal of Vibration Engineering & Technologies*, 7(6), 579–589. <https://doi.org/10.1007/s42417-019-00151-y>
- [16] D. L. Logan, *A First Course in the Finite Element Method*, 6th ed. Boston, MA, USA: Cengage Learning, 2012.
- [17] Timoshenko, S. P., 1921, "On the Correction for Shear of the Differential Equation for Transverse Vibrations of Prismatic Bars," *Philos. Mag.*, 41(245), pp. 744–746. <https://doi.org/10.1080/14786442108636264>
- [18] V. Giurgiutiu, *Stress, Vibration, and Wave Analysis in Aerospace Composites*. Amsterdam, Netherlands: Elsevier, 2022.
- [19] S. W. Doebling, C. R. Farrar, and M. B. Prime, "A summary review of vibration-based damage identification methods," *Shock Vib. Dig.*, vol. 30, no. 2, pp. 91–105, 1998. [Online]. Available: <https://doi.org/10.1177/058310249803000201>

- [20] A. D. Dimarogonas, "Vibration of cracked structures: A state of the art review," *Eng. Fract. Mech.*, vol. 55, no. 5, pp. 831–857, 1996. [Online]. Available: [https://doi.org/10.1016/0013-7944\(94\)00175-8](https://doi.org/10.1016/0013-7944(94)00175-8)
- [21] O. Daş, "Prediction of the natural frequencies of various beams using regression machine learning models," *Sigma J. Eng. Nat. Sci.*, vol. 41, pp. 302–321, 2023. [Online]. Available: <https://doi.org/10.14744/sigma.2023.00040>
- [22] Y. Jin and H. Su, "Machine learning models for predicting deflection and shape of 2D cantilever beams," in *Proc. ASME 2022 Int. Des. Eng. Tech. Conf. Comput. Inf. Eng. Conf.*, vol. 7: 46th Mechanisms and Robotics Conf., St. Louis, MO, USA, Aug. 14–17, 2022, V007T07A006.
- [23] "Crack detection in a cantilever beam using correlation model and machine learning approach," *Rom. J. Acoust. Vib.*, vol. 19, no. 2, pp. 121–133, Mar. 2023.
- [24] V. Khalkar, A. M. M. A. J. Decruz, L. Kamaraj, et al., "Damage identification in a cantilever beam using regression and machine learning models," *Iran J. Sci. Technol. Trans. Civ. Eng.*, vol. 48, pp. 4473–4488, 2024. [Online]. Available: <https://doi.org/10.1007/s40996-024-01563-x>
- [25] D. V. Ruiz, C. S. C. de Bragança, B. L. Poncetti, T. N. Bittencourt, and M. M. Futai, "Vibration-based structural damage detection strategy using FRFs and machine learning classifiers," *Structures*, vol. 59, 2024, Art. no. 105753. [Online]. Available: <https://doi.org/10.1016/j.istruc.2023.105753>
- [26] D. M. Onchis, "A deep learning approach to condition monitoring of cantilever beams via time-frequency extended signatures," *Comput. Ind.*, vol. 105, pp. 177–181, 2019. [Online]. Available: <https://doi.org/10.1016/j.compind.2018.12.005>
- [27] S. M. Haris and H. Mohammadi, "Cantilever Beam Natural Frequency Prediction Using Artificial Neural Networks," *Lecture notes in networks and systems*, pp. 441–449, Aug. 2017, doi: https://doi.org/10.1007/978-3-319-56991-8_33.